Inorg. Chem. **2003**, *42*, 6458–6468

Synthesis of a Pyridinium Bis[citrato(2−)]oxochromate(V) Complex and Its Ligand-Exchange Reactions

Carissa M. Cawich, Amritha Ibrahim, Karen L. Link, Allan Bumgartner, Mata D. Patro, and Surendra N. Mahapatro*

Department of Chemistry, Regis University, Denver, Colorado 80221

Peter A. Lay* and Aviva Levina

Centre for Heavy Metals Research, School of Chemistry, University of Sydney, New South Wales 2006, Australia

Sandra S. Eaton* and Gareth R. Eaton

Department of Chemistry and Biochemistry, University of Denver, Denver, Colorado 80208

Received February 11, 2003

The reaction of citric acid (caH_4) with pyridinium dichromate (PDC) in anhydrous acetone yields pyridinium bis[citrato(2−)]oxochromate(V), $pyH[CrO(caH_2)_2]$, as a mixed salt with the Cr(III) product. The compound persists in the solid state for months, is highly soluble in water (pH 4.0), and gives a sharp electron paramagnetic resonance (EPR) signal in solution ($g_{iso} = 1.9781$, $A_{iso}(Cr) = 17.1 \times 10^{-4}$ cm^{-1}), which is characteristic of d^1 Cr(V). The presence of $[Cr^{V}O(caH_2)_2]^-$ in the solid state was confirmed by electrospray mass spectroscopy, X-ray absorption near-edge structure (XANES), and EPR spectroscopy. Solid-state EPR spectroscopy, XANES, and a spectrophotometric assay showed that the solid is a mixture of $[Cr^{V}O(caH_2)_2]^-$ and a Cr(III)–citrate complex. The structures of the $[Cr^{V}O(caH_2)_2]^-$ and $[Cr^{III}(caH_2)_2]^-$ components of the mixture were established by multiple-scattering MS analysis of the X-ray absorption fine structure data. The structure of $[Cr^{V}O(caH_2)_2]^-$ is similar to that of other 2-hydroxy acid complexes with Cr═O, Cr—O(alcoholato), and Cr—O(carboxylato) bond lengths of 1.59, 1.81, and 1.90 Å, respectively. The Cr(III) complex has bond lengths typical for ligands with deprotonated carboxylate and protonated alcohol donors with distances of 1.90 and 1.99 Å, respectively, for the Cr—O(carboxylato) and Cr—O(alcohol) bond lengths. In aqueous solution, $[CrO(caH_2)_2]^-$ is short lived, but it is a convenient starting material for ligand-exchange reactions. It has been used to generate short-lived mixed-ligand Cr(V) complexes with citrate and picolinate, iminodiacetate, 2,2′-bipyridine, or 1,10-phenanthroline, which were characterized by EPR spectroscopy. The *g* values are between 1.971 and 1.974. For the picolinate, 2,2′-bipyridine, and 1,10-phenanthroline mixed-ligand complexes, there is hyperfine coupling (2.2×10^{-4} to 2.4×10^{-4} cm^{-1}) to a single proton of the citrate ligand.

Introduction

Since Roček and co-workers[1,2] discovered bis[2-ethyl-2-hydroxybutanoato(2−)]oxochromate(V), $[CrO(ehba)_2]^-$, and bis[2-hydroxy-2-methylbutanoato(2−)]oxochromate(V), $[CrO(hmba)_2]^-$, these complexes have served as model systems for studies of the structures and reactivities of Cr(V) complexes, as well as the mechanisms of Cr genotoxicity and Cr-induced cancers.[3−14] The Cr(V) and Cr(IV) complexes of ehba and hmba have sufficient stability to damage DNA in vitro at physiological pH values, even though they undergo rapid disproportionation reactions.[15]

* Authors to whom correspondence should be addressed. E-mail: smahapat@regis.edu (S.N.M.); p.lay@chem.usyd.edu.au (P.A.L.); seaton@du.edu (S.S.E.).

(1) Krumpolc, M.; DeBoer, B. G.; Roček, R. *J. Am. Chem. Soc.* **1978**, *100*, 145−153.
(2) Krumpolc, M.; Roček, J. *J. Am. Chem. Soc.* **1979**, *101*, 3206−3209.
(3) Gould, E. S. *Acc. Chem. Res.* **1986**, *19*, 72−77.
(4) Bose, R. N.; Fonkeng, B. S.; Moghaddas, S.; Stroup, D. *Nucleic Acids Res.* **1998**, *26*, 1588−1596.
(5) Sugden, K. D.; Wetterhahn, K. E. *Chem. Res. Toxicol.* **1997**, *10*, 1397−1406.

10.1021/ic034146l CCC: $25.00
Published on Web 09/10/2003

Neither ehba nor hmba is thought to have any cytosolic or mitochondrial biochemistry.[16]

Citric acid complexes of Cr(V) could provide a more relevant model for studies of Cr toxicity. Citric acid (caH_4) has diverse physiological roles in bacteria, as well as in higher organisms.[17] First, it is central to the citric acid cycle. Second, and potentially equally significant, citrate forms complexes with many metal ions, which increases solubility and leads to enhanced bioavailability and subsequent absorption by biological tissues.[18,19] A comprehensive study of the chromic acid oxidation of citric acid has been completed recently.[20] Even though citric acid forms a relatively stable and stoichiometric Cr(V) intermediate in chromic acid oxidations,[21,22] attempts to isolate an analogous Cr(V)−citrate complex following Roček's procedure[2] have not been successful to date. In this paper, the isolation and characterization of a citric acid complex of Cr(V) ($[Cr^{V}O(caH_2)_2]^-$), using pyridinium dichromate as the oxidant, is reported.

Ligand-exchange equilibria of oxalic acid or 1,2-ethanediol with $[CrO(ehba)_2]^-$ have been studied extensively,[14,23−28] and such ligand-exchange reactions are a prerequisite for electron transfer in the oxidation of organic substrates by Cr(V).[3,14,29−31] The unusual stability of $[CrO(ehba)_2]^-$ has allowed ligand-exchange reactions to be studied with oxygen[3,14,23−28,32,33] and sulfur donor ligands.[34] This is important because of the rapidly growing evidence that Cr(V) is the ultimate carcinogen,[4−9,14,15] and ligand-exchange studies at the Cr(V) center are critical to the understanding of Cr genotoxicity.[4,5,7,14,15] The Cr(V)−ehba complex undergoes direct ligand-exchange reactions with the DNA phosphate backbone, followed by hydrogen atom abstraction from a deoxyribose moiety.[4,7,15] Ligand-exchange reactions of Cr(V) and Cr(IV) intermediates, which are postulated to be involved in the picolinic acid (paH = pyridine-2-carboxylic acid) catalysis[35] of chromic acid oxidations of alcohols, are also likely to be important. However, stable picolinato complexes of Cr(V) or Cr(IV) have not been established[35] until recently, when a neutral bis(picolinato)oxochromium(IV) species was obtained through a ligand-exchange reaction of pa with $[CrO(ehbaH)_2]^0$.[36] The synthesis and characterization of Cr(III)−picolinate complexes are also of interest because of their use as dietary supplements.[37] The presence of mono-, bis-, and tris-pa−Cr(III) structures have been inferred from their ion-exchange behavior in aqueous solutions, but none of the species were initially isolated and characterized.[35] Subsequently, Cr−picolinate complexes were structurally characterized and they include $[Cr(pa)_3]$, $\{[Cr(pa)_2OH]_2\}$, and $[Cr_3O(paH)_6(H_2O)_3](ClO_4)_7$, but they are only slightly soluble in water (0.5−1 mM).[37] Because there are many potential N donors in biological systems and there is the possibility that Cr(V)- or Cr(IV)−pa complexes could be generated from Cr(III)-pa complexes, N-ligated oxochromium(V) systems are of considerable interest.[14] Such complexes, generated through the oxidation of Cr(III) chelates by phenyliodosoacetate,[38−41] PbO_2,[42,43] or IO_4^-,[42,43] damage DNA in vitro and are mutagenic to both bacterial and mammalian cells.[30,44,45] Chromium(V) peptide and amino acid complexes also have

(6) Barr-David, G.; Charara, M.; Codd, R.; Farrell, R. P.; Irwin, J. A.; Lay, P. A.; Bramley, R.; Brumby, S.; Ji, J.-Y.; Hanson, G. R. *J. Chem. Soc., Faraday Trans.* **1995**, *91*, 1207−1216.
(7) Farrell, R. P.; Judd, R. J.; Lay, P. A.; Dixon, N. E.; Baker, R. S. U.; Bonin, A. M. *Chem. Res. Toxicol.* **1989**, *2*, 227−229.
(8) Barr-David, G.; Hambley, T. W.; Irwin, J. A.; Judd, R. J.; Lay, P. A.; Martin, B. D.; Bramley, R.; Dixon, N. E.; Hendry, P.; Ji, J.-Y.; Baker, R. S. U.; Bonin, A. M. *Inorg. Chem.* **1992**, *31*, 4906−4908.
(9) Dillon, C. T.; Lay, P. A.; Bonin, A. M.; Dixon, N. E.; Collins, T. J.; Kostka, K. L. *Carcinogenesis* **1993**, *14*, 1875−1880.
(10) Zhitkovich, A.; Voitkun, V.; Costa, M. *Biochemistry* **1996**, *35*, 7275−7282.
(11) Lay, P. A.; Levina, A. *Inorg. Chem.* **1996**, *35*, 7709−7717.
(12) Chiu, A.; Chiu, N.; Shi, X.-L.; Beaubier, J.; Dalal, N. S. *Environ. Carcin. Ecotoxicol. Rev., J. Environ. Sci. Health, Part C* **1998**, *16*, 135−148.
(13) Zhang, L.; Lay, P. A. *J. Am. Chem. Soc.* **1996**, *118*, 12624−12637.
(14) Codd, R.; Dillon, C. T.; Levina, A.; Lay, P. A. *Coord. Chem. Rev.* **2001**, *216−217*, 537−582.
(15) (a) Levina, A.; Lay, P. A.; Dixon, N. E. *Inorg. Chem.* **2000**, *39*, 385−395. (b) Levina A.; Barr-David, G.; Codd, R.; Lay, P. A.; Dixon, N. E.; Hammershøi, A.; Hendry, P. *Chem. Res. Toxicol.* **1999**, *12*, 371−381.
(16) Koolman, J.; Röhm, K.-H. *Color Atlas of Biochemistry*; Thieme Medical Publishers: New York, 1996.
(17) (a) Glusker, J. P. *Acc. Chem. Res.* **1980**, *13*, 354−352. (b) Martin, R. B. *J. Inorg. Biochem.* **1986**, *28*, 181−187.
(18) Beinert, H.; Kennedy, M. C. *Eur. J. Biochem.* **1989**, *186*, 5−15.
(19) Baker, E. N.; Baker, H. M.; Anderson, B. F.; Reeves, R. D. *Inorg. Chim. Acta* **1983**, *78*, 282−285.
(20) Bumgartner, A.; Ibrahim, A.; Patro, M. D.; Mahapatro, S. N.; Samal, P. C.; Pattnaik, B. B.; Lay, P. A., Levina, A. *Inorg. Chem.*, submitted.
(21) Kon, H. *Bull. Chem. Soc. Jpn.* **1962**, *35*, 2054−2055.
(22) Kon, H. *J. Inorg. Nucl. Chem.* **1963**, *25*, 933−944.
(23) Bramley, R.; Ji, J.-Y.; Lay, P. A. *Inorg. Chem.* **1991**, *30*, 1557−1564.
(24) Farrell, R. P.; Judd, R. J.; Lay, P. A.; Bramley, R.; Ji, J.-Y. *Inorg. Chem.* **1989**, *28*, 3403−3410.
(25) Farrell, R. P.; Lay, P. A.; Levina, A.; Maxwell, I. A.; Bramley, R.; Brumby, S.; Ji, J.-Y. *Inorg. Chem.* **1998**, *37*, 3159−3166.
(26) Farrell, P. R.; Lay, P. A. *Comments Inorg. Chem.* **1992**, *13*, 133−175.
(27) Branca, M.; Dessi, A.; Micera, G.; Sanna, D. *Inorg. Chem.* **1993**, *32*, 578−581.
(28) Branca, M.; Micera, G.; Serge, U.; Dessi, A. *Inorg. Chem.* **1992**, *31*, 2404−2408.
(29) Headlam, H. A.; Lay, P. A. Personal communication.
(30) Headlam, H. A., Ph.D. Thesis, University of Sydney, 1999.
(31) Krumpolc, M.; Roček, J. *Inorg. Chem.* **1985**, *24*, 617−621.
(32) Bramley, R.; Ji, J.-Y.; Judd, R. J.; Lay, P. A. *Inorg. Chem.* **1991**, *30*, 3089−3094.
(33) Codd, R.; Lay, P. A. *J. Am. Chem. Soc.* **1999**, *121*, 7864−7876.
(34) Ghosh, S.; Bose, R.; Gould, E. S. *Inorg. Chem.* **1987**, *26*, 3722−3727.
(35) Roček, J.; Peng, T.-Y. *J. Am. Chem. Soc.* **1977**, *99*, 7622−7631.
(36) Codd, R.; Lay, P. A.; Levina, A. *Inorg. Chem.* **1997**, *36*, 5440−5448.
(37) (a) Stearns, D. M.; Armstrong, W. H. *Inorg. Chem.* **1992**, *31*, 5178−5184 and references therein. (b) Bradshaw, J. E.; Grossie, D. A.; Mullica, D. F.; Pennington, D. E. *Inorg. Chim. Acta* **1988**, *141*, 41−47. (c) Evans, G. W. Dietary Supplementation with Essential Metal Picolinates. U.S. Patent 4,315,927, 1981.
(38) Siddall, T. L.; Miyaura, N.; Huffmann, J. C.; Kochi, J. K. *J. Chem. Soc., Chem. Commun.* **1983**, 1185−1186.
(39) Collins, T. J.; Slebodnick, C.; Uffelman, E. S. *Inorg. Chem.* **1990**, *29*, 3433−3436.
(40) Samsel, E. G.; Srinivasan, K.; Kochi, J. K. *J. Am. Chem. Soc.* **1985**, *107*, 7606−7617.
(41) Groves, J. T.; Takahashi, T.; Butler, W. *Inorg. Chem.* **1983**, *22*, 884−887.
(42) Sulfab, Y.; Al-Shatti, N. I.; Hussein, M. A. *Inorg. Chim. Acta* **1984**, *86*, L59−L60. This complex was initially characterized as a periodato complex of Cr(V) but was later characterized as *cis*-$[Cr(phen)_2(O)_2]^+$ and can be generated by either the PbO_2 or IO_4^- oxidation of *cis*-$[Cr(phen)_2(OH_2)_2]^{3+}$ (Sulfab, Y.; Nasreldin, M. *Transit. Met. Chem.* **2001**, *26*, 147−149; Dillon, C. T. Ph.D. Thesis, University of Sydney, 1995).
(43) Headlam, H. A.; Lay, P. A. *Inorg. Chem.* **2001**, *40*, 78−86.
(44) Dillon, C. T.; Lay, P. A.; Bonin, A. M.; Cholewa, M.; Legge, G. J. F. *Chem. Res. Toxicol.* **2000**, *13*, 742−748.
(45) Dillon, C. T.; Lay, P. A.; Bonin, A. M.; Dixon, N. E.; Sulfab, Y. *Aust. J. Chem.* **2000**, *53*, 411−424.

been prepared by ligand-exchange reactions of Cr(V) methanol complexes with peptides or amino acids.[30,43,46] Here the ligand-exchange reactivity of the Cr(V)−citrate complex (which is more labile than the much-studied ehba analogue) is reported for the ligands picolinate, iminodiacetate, 2,2′-bipyridine, and 1,10-phenanthroline.

Experimental Section

$Na[Cr(ehba)_2]$ was synthesized from 2-ethyl-2-hydroxybutanoic acid (Aldrich 99%) and sodium dichromate (Merck) in anhydrous acetone (Aldrich 99.9%) according to the literature method.[2] Anhydrous citric acid (Aldrich 99%), picolinic acid (Aldrich 99%), 2,2′-bipyridine (Aldrich 98%), 1,10-phenanthroline (Aldrich, 98%), and iminodiacetic acid (Aldrich 97%) were used without further purification. Aldrich molecular sieves (5 Å) were activated by heating for 6 h at 180−200 °C under vacuum.

Ring-deuterated picolinic acid (D_4C_5NCOOH) was prepared by $KMnO_4$ oxidation of perdeuterated 2-picoline ($D_4C_5NCD_3$, Aldrich sample 98% D) by following the procedure described for the synthesis of picolinic acid.[47]

Caution. Cr(VI) complexes are carcinogenic,[48] and Cr(V) complexes are known mutagens.[7,9,14] Care must be taken to avoid skin contact and inhalation of dusts.

Synthesis of Cr(V/III)−Citrate (I and II). Anhydrous citric acid (5.76 g, 0.03 mol) was dissolved in anhydrous acetone (160 mL). Pyridinium dichromate (1.88 g, 5 mmol, 10 mmol in Cr(VI)) was added, and the reaction mixture was stirred in the presence of 5-Å molecular sieves (10 g) for 1 h. With the dissolution of pyridinium dichromate, the color changed from the orange dichromate to a red-brown due to the formation of the Cr(V) complex. The solution became heterogeneous, and a brown solid precipitated. Most of the molecular sieves settled to the bottom of the reaction flask. The contents were swirled, and the Cr(V)−Cr(III) solid was filtered with care in order to leave the molecular sieves in the flask. Occasionally one or two molecular sieves got on to the filter paper and were removed by a spatula or glass rod. The solid was rinsed with dry acetone followed by anhydrous hexane and was dried in a vacuum, yield 3.0 g. The solid is highly soluble in water, DMF, and DMSO but is only sparingly soluble in acetone, methanol, ethanol, and THF. The solid was stored desiccated at 4 °C.

$(pyH)_2[Cr(caH_2)_2]\cdot 4H_2O$ was prepared by the literature method[49] and was characterized by electron paramagnetic resonance (EPR) and visible spectra.

Determination of total Cr by atomic absorption spectroscopy (AAS) was performed using a C_2H_2/air flame on a Varian SpecAA-800 spectrometer. The sample (20.0 mg) was digested in 70% HNO_3 (∼1 mL) and diluted with 0.1 M HCl to 5.0 mL. This solution was diluted 100 times with 0.1 M HCl for AAS measurements. Found: [Cr] = 9.1−10.6% Cr by weight. The % Cr calculated for a 1:1 mixture of **I** ($C_{17}CrH_{18}NO_{15}$) and **II** ($C_{17}CrH_{17}NO_{14}$) is based on a molecular formula of $C_{34}Cr_2H_{35}N_2O_{29}$ (calculated C, 39.2, Cr, 10.0; H, 3.37; N, 2.69; O, 44.6. Found: C, 38.8, Cr, 9.1−10.6; H, 3.9; N, 3.3; O, 42.8). The uncertainty in % O may have resulted from an additional amount of water (not determined) in the Cr(III) species.[49] Elemental analyses were performed by Huffman Laboratories, Golden, CO.

Cr Oxidation State. The average formal oxidation state of Cr was determined by a spectrophotometric method. Weighed samples (10−20 mg) were dissolved in 0.5 M NaOH (50−60 mL) and heated to 80 °C (15 min). The samples were cooled to room temperature and diluted to a total volume of 100 mL with deionized water in standard volumetric flasks. The absorbance due to CrO_4^{2-} at 372 nm was measured. The samples were then treated with excess H_2O_2 (Aldrich, 30%), heated to boiling (in order to decompose the excess H_2O_2), and made up to the same total volume at room temperature. Final absorbance values (after H_2O_2 oxidation) were recorded at the same wavelength. Chromium(III) has a negligible contribution to the absorbance at 372 nm.

Electrospray Mass Spectrometry (ESMS). The ESMS analyses were performed using a Finnigan LSQ mass spectrometer. Typical experimental settings were as follows: sheath gas (N_2) pressure, 60 psi; spray voltage, 5.0 kV; capillary temperature, 200 °C; capillary voltage, 19 V; tube lens offset, 25 V; and *m*/*z* range, 100−1000 both in positive- and negative-ion modes. Analyzed solutions (1.0 mg/mL sample in DMF or H_2O; reaction time ∼1 min at 22 °C) were injected into a flow of 50% (v/v) MeOH/H_2O (flow rate 0.20 mL/min). Acquired spectra were the averages of 10 scans (scan time 10 ms). Simulations using IsoPro software[50] were used to confirm the assignments of the signals.

X-ray Absorption Spectroscopy (XAS). Chromium K-edge XAS spectra were recorded on the Australian National Beamline Facility (Beamline 20B) at the Photon Factory, Tsukuba, Japan. The beam energy was 2.5 GeV, and the beam current was 300−400 mA. A Si[111] double-crystal monochromator was detuned by 50%. The spectra were recorded in transmission mode, using standard N_2-filled ionization chambers. The powdered samples were mixed with BN (mass ratio 1:1) and pressed into 0.5-mm pellets supported in an Al spacer between two 63.5-μm Kapton tape windows. The sample temperature was maintained at 10 K, using a closed-cycle He CryoIndustries REF-1577-D22 cryostat. The low temperature used for data collection minimized photodamage and improved the signal-to-noise ratio.[51] The spectra were averaged from two scans taken at different positions on the sample, and the edge energies differed by <0.1 eV between the scans. The energy scale was calibrated using a Cr foil as an internal standard (calibration energy, 5989.0 eV, corresponded to the first peak of the first derivative of the Cr(0) edge).[52]

Averaging, background subtraction, and the calculation of theoretical X-ray absorption fine structure (XAFS) spectra were performed using the XFIT software package,[53] including the multiple-scattering (MS) FEFF 6.01 algorithm,[54] as described previously.[51,55,56] The model (Chart S1 in Supporting Information

(46) Headlam, H. A.; Weeks, C. L.; Hambley, T. W.; Turner, P.; Lay, P. A. *Inorg. Chem.* **2001**, *40*, 5097−5105.
(47) Singer, A. W.; McElvain, S. M. *Organic Synthesis Collective;* Horning, E. C., Ed. John Wiley & Sons: New York, 1955; Vol. 3, pp 740−741.
(48) *IARC. Monographs on the Evaluation of the Carcinogenic Risk of Chemicals to Humans Chromium, Nickel and Welding*; Vol. 49, IARC: Lyon, France, 1990.
(49) Quiros, M.; Goodgame, D. M. L.; Williams, D. J. *Polyhedron* **1992**, *11*, 1343−1348.
(50) Senko, M. *IsoPro 3.0*; Sunnyvale, CA, 1998.
(51) (a) Rich, A. M.; Armstrong, R. S.; Ellis, P. J.; Freeman, H. C.; Lay, P. A. *Inorg. Chem.* **1998**, *37*, 5743−5753. (b) Rich, A. M.; Armstrong, R. S.; Ellis, P. J.; Lay, P. A. *J. Am. Chem. Soc.* **1998**, *120*, 10827−10836.
(52) Arèon, I.; Mirtič, B.; Kodre, A. *J. Am. Ceram. Soc.* **1998**, *81*, 222−224.
(53) (a) Ellis, P. J.; Freeman, H. C. *J. Synchrotron Radiat.* **1995**, *2*, 190−195. (b) *XFIT for Windows95;* Australian Synchrotron Research Program: Sydney, Australia, 1996.
(54) Rehr, J. J.; Albers, R. C.; Zabinsky, S. I. *Phys. Rev. Lett.* **1992**, *69*, 3397−3400.
(55) Codd, R.; Levina, A.; Zhang, L.; Hambley, T. W.; Lay, P. A. *Inorg. Chem.* **2000**, *39*, 990−997.
(56) Levina, A.; Foran, G. J.; Lay, P. A. *J. Chem. Soc., Chem. Commun.* **1999**, 2339−2340.

(SI)) included two first shells, as well as O atoms of the third shells, for the expected structures of $[Cr^{V}O(caH_2)]^-$ and $[Cr^{III}(caH)(caH_2)]^{2-}$. A model of $[Cr^{V}O(ehba)_2]^-$, optimized by molecular mechanics calculations,[55,57,58] was used as an initial model for $[Cr^{V}O(caH_2)]^-$, while an initial model for $[Cr^{III}(caH)(caH_2)]^{2-}$ was built using HyperChem software.[59] No attempts were made to model other geometric isomers of the Cr(V) or Cr(III) complexes, since changes in the geometric isomers have only a small effect on the results of MS XAFS calculations,[55,57] and these could not be distinguished with certainty in a two-site model. The two Cr centers were placed at a distance of 10 Å, which excluded their interaction or significant multiple-scattering contributions from the ligands of the second complex to the first and vice versa (maximal path length of a photoelectron was set at 5.0 Å). Conditions, restraints, and constraints, applied to the MS XAFS calculation for the Cr(V)−Cr(III)−citrate model, are listed in Tables S1 and S2 in SI, and the applied Fourier transform (FT) window function is shown in SI Figure S1. The value of threshold energy (approximately equal to that of the edge energy in X-ray absorption near edge structure (XANES) spectra)[53] for the Cr(III) complex was restrained to be 2.5 ± 1.0 eV lower than the corresponding value for the Cr(V) complex, in agreement with the data for Cr(III)- and Cr(V)−ehba complexes.[56,57] The occupancies (*N*) for all the atoms of the Cr(V) or Cr(III) complexes were constrained to be equal and the sum of *N*(Cr(V)) and *N*(Cr(III)) was constrained to be equal to 1; the initial *N* values for all atoms were set at 0.5. The Debye−Waller factors of the similar atoms in the Cr(V) and Cr(III) complexes were restrained to be close (within 0.001 $Å^2$), and those of the equal atoms of the two ligands (in either Cr(V) or Cr(III) complexes) were constrained to be equal to reduce the number of variables. The Cr−O bond lengths for the oxo, carboxylato, or alcoholato ligands were restrained to be close (within 0.05 or 0.1 Å) to the corresponding values in the $[Cr^{V}O(ehba)_2]^-$ [60] and $[Cr^{III}(caH)(caH_2)]^{2-}$ complexes.[49] Bond lengths and angles in the ligands were restrained to be close (within 0.05 Å or 5°) to those for the corresponding hybridization states of the C atoms (sp^3 or sp^2);[55] these values were also in agreement with the crystal structures of $[Cr^{V}O(ehba)_2]^-$ and $[Cr^{III}(caH)(caH_2)]^{2-}$.[49,60] Bond angles between the ligands were not restrained.[55,57] The overdeterminacy of the applied model (N_i/p = 1.1, where N_i is the number of independent observations and *p* is the number of varied parameters) was checked by the method of Binsted et al.,[61] taking into account the applied restraints and constraints. The random errors in the estimated XAFS parameters, arising from the noise in the data, were determined by Monte Carlo analysis within the XFIT software[53] and did not exceed the limits of expected systematic errors of MS XAFS calculations (±0.02 Å for the bond lengths and ±2° for the bond angles).[62]

EPR Spectroscopy at the University of Sydney. X-Band EPR spectra of the Cr(V/III)−citrate complex were recorded using a quartz capillary (for the solid) or a flat quartz cell (for the 1.0 mg/mL solutions in DMF or in H_2O) on a Bruker EMX spectrometer equipped with a Bruker EMX 035M NMR gaussmeter and a Bruker EMX048T microwave frequency counter. The instrument settings were as follows: center field, 3500 G; sweep width, 1000 G (for the solid) or 100 G (for the solutions); resolution, 1024 points; microwave frequency, ~9.66 GHz; microwave power, 2.0 mW; modulation frequency, 100 kHz, modulation amplitude, 0.97 G; time constant, 0.64 ms; sweep time, 5.24 s; receiver gain, 1×10^3 to 5×10^4; and number of scans, 5. All spectra were recorded at 22 °C. The EPR spectra were processed using WIN-EPR software.[63] Second-order corrections were applied in determining the EPR spectral parameters.

For EPR quantification of Cr(V) in the solid sample used for the XAS experiments, areas of the EPR signals (determined by WinEPR software[63]) were used for calibration. Reproducibility of results was achieved by keeping a constant *Q* value (1100 ± 100), which is a measure of the EPR cell position in the cavity.[64] Calibration was performed using a 20.0 mM solution of $Na[Cr^{V}O(ehba)_2]$ in DMF. This solution (0.5−5.0 μL) was added to $ehbaH_2$/ehbaH buffer (0.50 mL, 100 mM, pH 3.5), and EPR spectra were taken within 3 min. The calibration was linear for [Cr(V)] over the range of 0.02−0.20 mM (second integral = (62 ± 2)[Cr(V)], R = 0.998). Determination of [Cr(V)] in the Cr(V/III)−citrate sample was performed by the standard addition method. The sample (10.0 mg) was dissolved in DMF (1.0 mL), and 5.0 μL of this solution, together with 0−1.5 μL of $Na[Cr^{V}O(ehba)_2]$ solution (20.0 mM) in DMF, was added to 0.50 mL of ehba buffer solution (100 mM, pH 3.5). As discussed below, the Cr(V)−citrate complex rapidly converts to $[CrO(ehba)_2]^-$ under these conditions. The determination of the double-integrated intensities of EPR signals gave a straight line with the same slope as the calibration line (second integral = (2.35 ± 0.04) + (60 ± 1)[Cr(V)], R = 0.999). The results of two independent determinations agreed within 5%. From these data, the Cr(V) content in the solid sample was 2.08%, i.e., 20% of the total Cr. However, this may be an underestimation, as a part of Cr(V)−citrate may be reduced in the ehba buffer parallel to the conversion to $[Cr^{V}O(ehba)_2]^-$. The stability of the Cr(V)−citrate complex in DMF solution was also checked by this method. During the time required for one experimental series (~20 min), the amount of Cr(V)−citrate in DMF solutions decreased by ~8%. In contrast, $[Cr^{V}O(ehba)_2]^-$ is stable for days in DMF solution.[55]

EPR Spectroscopy at the University of Denver. X-Band (9.1 to 9.2 GHz) EPR spectra of ligand-exchange reactions and solids were run on a Varian E9 spectrometer on solutions contained in 1-mm i.d. capillaries or solids in quartz tubes. Spectra at 35 GHz were obtained on a modified Varian Q-band spectrometer[65] on samples in ~0.4-mm i.d. quartz capillaries. Spectra at 1.5 GHz were obtained on a locally constructed system[66] on samples in ~1-mm i.d. quartz capillaries. At each of the microwave frequencies, the magnetic field modulation frequency was 100 kHz. Values of *g* and hyperfine-coupling constants were determined by computer simulation using locally written programs for fluid solution (Epr2) (uncertainty in *g* values is about ±0.0003) and rigid lattices (Monmer)[67] that include second-order corrections to the hyperfine interaction.

The Cr(V) content of the isolated solid was quantified (after fast ligand exchange) by comparing the normalized EPR double integral of a 1 mg mL^{-1} solution of the isolated solid in $ehbaH_2$/ehbaH

(57) Levina, A.; Lay, P. A.; Codd, R.; Foran, G. J.; Hambley, T. W.; Maschmeyer, T.; Masters, A. F. *Inorg. Chem.*, submitted.
(58) Codd, R. BSc(Hons) Thesis. University of Sydney, Sydney, 1992.
(59) *HyperChem*, *Version 5.1*; Hypercube Inc.: Gainesville, FL, 1996.
(60) Judd, R. J.; Hambley, T. W.; Lay, P. A. *J. Chem. Soc., Dalton Trans.* **1989**, 2205−2210.
(61) Binsted, N.; Strange, R. W.; Hasnain, S. S. *Biochemistry* **1992**, *31*, 12117−12125. The overdeterminacy of the model (N/p > 1) is required to obtain a meaningful solution from XAFS spectra fitting.
(62) Gurman, S. J. *J. Synchrotron Radiat.* **1995**, *2*, 56−63.
(63) *WIN-EPR, Version 921201*; Bruker-Franzen Analytic: Bremen, Germany.
(64) Weber, R. T. *EMX User's Manual*; Bruker Instruments: Billerica, MA, 1995.
(65) Eaton, S. S.; More, K. M.; Dubois, D. L.; Boymel, P. M.; Eaton, G. R. *J. Magn. Reson.* **1980**, *41*, 150−157.
(66) Quine, R. W.; Rinard, G. A.; Ghim, B. T.; Eaton, S. S.; Eaton, G. R. *Rev. Sci. Instrum.* **1996**, *67*, 2514−2527.
(67) Toy, A. D.; Chaston, S. H. H.; Pilbrow J. R.; Smith, T. D. *Inorg. Chem*. **1971**, *10*, 2219−2225.

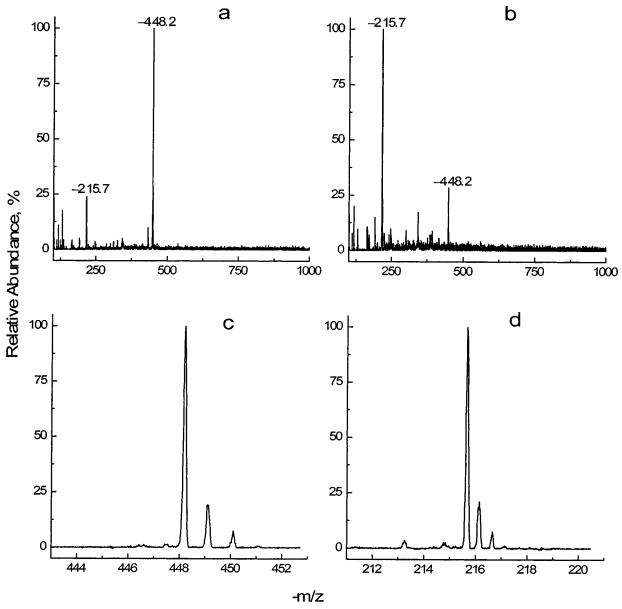

Figure 1. Typical electrospray mass spectra (negative-ion mode) of Cr(V/III)−citrate solutions (1.0 mg mL^{-1}) in (a) DMF or (b) H_2O (pH 4.0) and expansions of signals of (c) $[Cr^{V}O(caH_2)_2]^-$ and (d) $[Cr^{III}(caH)(caH_2)]^{2-}$.

buffer to that of a gravimetrically prepared solution of *tempone* (Aldrich Chemical, 99%). The Cr(V) concentration varied from batch to batch and decreased as a function of time between preparation of the Cr(V/III)−citrate complex and the EPR assay. The Cr(V)−citrate complex comprised 25−35% of the original solid.

Ligand-Exchange Studies. Solutions (20−100 mM) of the appropriate ligand were prepared by dissolving weighed amounts of the ligands in doubly distilled water and then titrating them to the desired pH values (3.0−4.5). An aqueous solution of picolinate was titrated to the desired pH value (4.0−4.5) with NaOH. Solutions of 2,2′-bipyridine and 1,10-phenanthroline were titrated with $HClO_4$ to pH 4.1 ± 0.1. Ligand-exchange reactions were initiated by dissolving the solid Cr(V/III)−citrate compound in the appropriate ligand-containing buffered solution (1 mg of the Cr(V/III) complex per mL of buffer). Initial EPR spectra of the solutions were recorded within 4 min of dissolution, and changes in spectra as a function of time were monitored. After completion of the ligand-exchange reactions with picolinic acid, ESMS spectra were recorded.

Results

Characterization of the Cr(V/III)−Citrate Complex. Typical negative-ion ESMS spectra of the citrate complex are shown in Figure 1. The predominant Cr-containing species are $[Cr^{V}O(caH_2)_2]^-$, $[Cr^{III}(caH)(caH_2)]^{2-}$, and $[HCr^{VI}O_4]^-$ (Table 1). The relative abundance of Cr(V) compared to Cr(III) and Cr(VI) is lower in H_2O (pH = 4.0) than in DMF, which implies that $[Cr^{V}O(caH_2)_2]^-$, analogous to $[Cr^{V}O(ehba)_2]^-$ and $[Cr^{V}O(qa)_2]^-$ (qa = quinato(2−)), is more stable in DMF than in aqueous solutions.[55] The presence of a $[HCr^{VI}O_4]^-$ signal in a freshly prepared DMF solution may mean that the solid sample contained some Cr(VI) in addition to Cr(III) and Cr(V) or more likely that some Cr(V) disproportionated to form Cr(VI) in the aqueous methanol used in the injection. No significant Cr-containing signals were observed in the positive-ion mode (either in DMF or in H_2O).

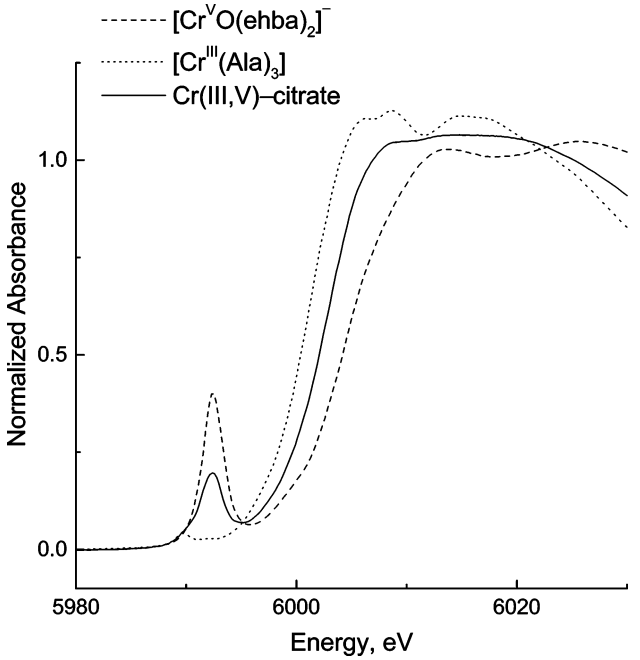

Figure 2. XANES spectra of Cr(V/III)−citrate and reference compounds (solid state, 10 K). See text for experimental details.

Table 1. Summary of Negative-Ion ESMS Results

		relative abundance, %	
assignment	−*m*/*z*	in DMF	in H_2O (pH 4)
$[HCr^{VI}O_4]^-$	117.0	9	20
caH_3^-	191.1	4	16
$[Cr^{III}(caH)(caH_2)]^{2-}$	215.7	23	100
$[Cr^{III}(caH_2)_2]^-$	432.2	9	
$[Cr^{V}O(caH_2)_2]^-$	448.2	100	30

The K-edge XANES spectrum of the Cr(V/III)−citrate sample is shown in Figure 2 along with spectra of a Cr(V) standard ($Na[Cr^{V}O(ehba)_2]$[56,57]) and a Cr(III) standard ($[Cr^{III}(Ala)_3]$[68]). The spectrum of the Cr(V/III)−citrate complex has features similar to both standards. Two pre-edge features due to 1s → 3d transitions are a weak peak at 5989.6 eV and a stronger peak at 5992.4 eV. The positions and the intensities of these peaks are typical of 2-hydroxy acid complexes of Cr(III) and Cr(V), respectively,[56,57] and hence the XANES spectrum indicates that the solid is a mixture of Cr(V) and Cr(III) complexes. From the intensities of the pre-edge peaks and the edge positions, the Cr(V) content of the Cr(V/III)−citrate sample was estimated to be of the order of ∼35−45% of Cr, which was a little higher than that estimated by the XAFS analysis and EPR spectroscopy.

A summary of the MS XAFS fitting results is given in Table 2, and a detailed list of initial, restrained, and optimized parameters is given in SI Table S2. The optimized fit (Figure 3) is consistent with the mixture of 26% of Cr(V) and 74% of Cr(III) complexes, in good agreement with the EPR data (see below). The Cr−O bond lengths in the Cr(V)−citrate complex are similar to the corresponding values for $[Cr^{V}O(ehba)_2]^-$,[60] except for a slightly longer Cr−O(oxo) bond (1.59 vs 1.56 Å). The optimized Cr−O bond lengths

(68) The complex was prepared according to the method described by Murdoch, C. M. Ph.D. Thesis, University of Sydney, 1988.

Table 2. Summary of XANES Data and MS XAFS Fitting Results for the Cr(V)−Cr(III)−Citrate Mixture (solid, 10 K)

	values[a]	
parameter	Cr(V)	Cr(III)
XANES parameters		
pre-edge transitions, eV	5992.4, 5989.6 (shoulder)	
edge energy, eV	6002.0	
XAFS parameters		
GOF, R %[b]	13.8	
occupancy	0.26[d]	0.74[d]
threshold energy, eV	6003.8(2)	6001.4(3)
scale factor, S_0^2 [c]	0.91(1)	0.92(1)
optimized Cr−O bond lengths, Å		
oxo	1.59(1)	- -
carboxylato	1.90(1)	1.90(1)
alcoholato/alcohol	1.81(1)	1.99(1)
Debye−Waller factors, Å^2		
O (oxo)	0.0010(1)	
O (carboxylato)	0.0013(1)	0.0013(1)
O (alcoholato)	0.0010(1)	0.0010(1)

[a] Errors in the last significant digit (calculated by the Monte Carlo method)[53] are given in parentheses. [b] Smaller R values correspond to a better fit; fits with $R < 20\%$ are considered good.[61] [c] Acceptable values for this factor are 0.9 ± 0.1.[53] [d] The errors in these values could not be determined, as their sum was constrained to be equal to 1.

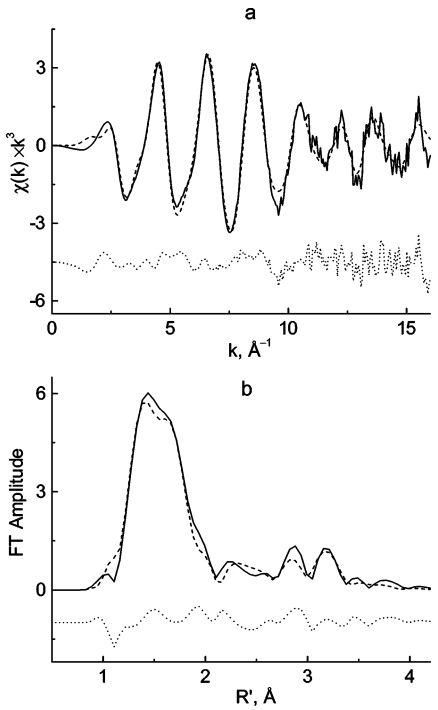

Figure 3. Experimental (solid lines) and calculated (dashed lines) XAFS (a) or FT XAFS (b) spectra of the Cr(V)−Cr(III)−citrate mixture (10 K). Fit residuals are shown by dotted lines. For FT XAFS, both experimental and calculated spectra are windowed; applied window functions are shown in SI Figure S1.

in the Cr(III)−citrate complex are consistent with the binding of four carboxylato groups (1.90 Å) and two ROH groups (1.99 Å).[56,57] The latter value is somewhat higher, but not significantly so, than that for the "half-protonated" alcoholato groups in the crystal structure of $[Cr^{III}(caH)(caH_2)]^{2-}$ (1.96 Å).[49] Thus, the major Cr(III) component of the solid Cr(V)−Cr(III)−citrate mixture is likely to be $[Cr^{III}(caH_2)_2]^-$.

A 1000-G scan of the EPR spectra of freshly prepared

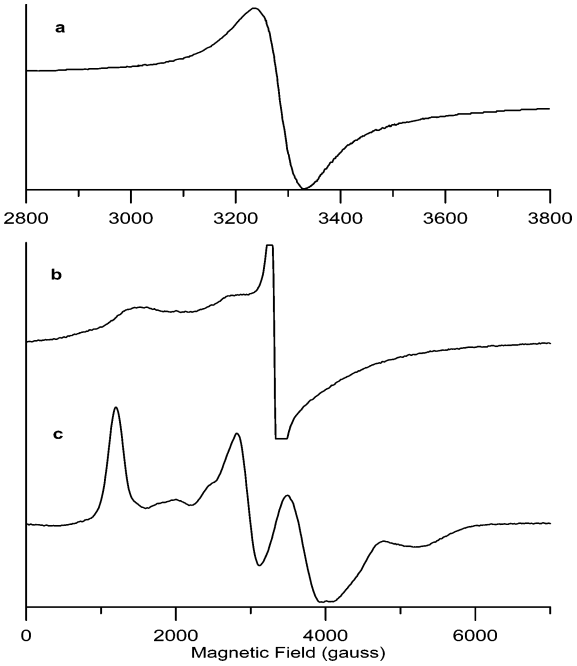

Figure 4. Room-temperature continuous-wave X-band EPR spectra of solid samples obtained with a microwave power of 12.5 mW and a modulation amplitude of 5 G: (a) 1000-G scan (9.1053 GHz) of Cr(V/III)−citrate, (b) 7000-G scan (9.1760 GHz) of Cr(V/III)−citrate recorded at higher amplification to emphasize broad underlying signals, and (c) 7000-G scan (9.1760 GHz) of $(pyH)_2[Cr(caH_2)_2]\cdot 4H_2O$.[49]

solid Cr(V/III)−citrate (Figure 4a) showed a 100-G wide line with $g = 1.98$, which is assigned as Cr(V) based on the g value. A wider scan, at higher gain (Figure 4b), revealed additional signals extending over thousands of gauss. For comparison, the spectrum from a solid sample of the Cr(III)−citrate complex $(pyH)_2[Cr(caH_2)_2]\cdot 4H_2O$ that was isolated from the reaction of citric acid with pyridinum dichromate in aqueous medium[49] is shown in Figure 4c. The features in the spectrum of solid Cr(V/III)−citrate occur over a range of magnetic fields that is similar to that for authentic $(pyH)_2[Cr(caH_2)_2]\cdot 4H_2O$, which is consistent with assignment of these features in the spectrum of Cr(V/III)−citrate solid to a Cr(III) citrate complex.

When the solid Cr(V/III)−citrate sample is dissolved in water, a characteristic d^1 Cr(V) spectrum is observed. A sharp signal with $g_{iso} = 1.9781$ (in either DMF or H_2O) is due to isotopes with $I = 0$ (^{50}Cr, ^{52}Cr, ^{54}Cr), which constitute 90.5% of natural abundance. In addition, there are satellite lines due to ^{53}Cr ($I = {}^3/_2$, 9.5% natural abundance), which have $A_{iso} = 16.6 \times 10^{-4}$ cm^{-1} (in DMF) or 17.1×10^{-4} cm^{-1} (in H_2O). Unlike $[Cr^{V}O(ehba)_2]^-$ or $[Cr^{V}O(qa)_2]^-$, no evidence for geometric isomerism was revealed in the EPR spectra of $[Cr^{V}O(caH_2)_2]^-$.[33] For an aqueous solution with a concentration ~1 mg mL^{-1} at pH 4, the signal decays to 20% of original intensity within 60 min. The stability decreases in the following order: aqueous solution (pH 4) > 0.1 M $HClO_4$ (pH 1.0) > 0.1 M citrate buffer (pH 3−4) > acetate buffer (pH 4.5) > phosphate buffer pH 7.0.

A spectrophotometric assay was performed by monitoring the $[CrO_4]^{2-}$ absorbance at 372 nm in alkaline medium (0.5 M NaOH) before and after H_2O_2 oxidation. In alkaline

medium, Cr(V) disproportionates to a 2:1 mixture of $[CrO_4]^{2-}$ and Cr(III) as shown in eq 1.

$$3Cr(V) \rightarrow 2Cr(VI) + Cr(III) \quad (1)$$

Addition of alkaline H_2O_2 converted the Cr(III) to $[CrO_4]^{2-}$. Thus, for a pure Cr(V) complex, the characteristic $[CrO_4]^{2-}$ absorbance at 372 nm after addition of alkaline H_2O_2 would be 1.5 times as large as that observed for a disproportionated sample before addition of H_2O_2. For solutions prepared from solid samples of Cr(V/III)−citrate, the absorbance at 372 nm after addition of H_2O_2 was 3−3.5 times as large as in the disproportionated solution before addition of H_2O_2, which suggests an approximately equimolar mixture of Cr(III) and Cr(V) in the solid. This method only gives semiquantitative results because of the competing reduction of Cr(VI) by H_2O_2.[69]

Ligand-Exchange Studies. When the Cr(V/III)−citrate complex was dissolved in a buffered ehbaH/ehbaH_2 solution, the characteristic Cr(V) EPR signal did not decrease over a 24-h period, indicating that the ligand-exchange reaction to form the more stable $[CrO(ehba)_2]^-$ complex (eq 2; ehbaH and CaH_3 denote the 1^- anions of ehbaH_2 and ehbaH_4, respectively) was essentially complete within the few minutes between mixing the solutions and recording the EPR spectrum. The resulting $[CrO(ehba)_2]^-$ signal was used to quantify the Cr(V) in the solid by EPR spectroscopy. The values of ∼25−35% were consistent with those obtained from the XANES and XAFS results.

$$[CrO(caH_2)_2]^- + 2\ ehbaH \rightarrow [CrO(ehba)_2]^- + 2\ caH_3 \quad (2)$$

The X-band spectrum of Cr(V/III)−citrate plus picolinic acid in H_2O or DMSO is a four-line spectrum (Figure 5) due to the exchange of 1 mol of citrate with 1 mol of picolinate (eq 3).

$$[CrO(caH_2)_2]^- + paH \rightarrow [CrO(caH)(pa)]^- + caH_3 + H^+ \quad (3)$$

Coupling to the picolinate nitrogen ($I = 1$) would give a three-line spectrum. A four-line pattern could result from an additional coupling to a single proton or to overlapping signals from two species with slightly different g values, as is observed for the mixture of cis and trans isomers of $[CrO(ehba)_2]^-$,[32,33] $[CrO(hmba)_2]^-$,[33,60] $[CrO(qaH_3)_2]^-$,[33,55] and $[Cr(NO)(ehba)_2]$.[70] To distinguish between these two possibilities, spectra were obtained at additional microwave frequencies. The $[CrO(caH)(pa)]^-$ complex is more stable in DMSO solution than in water; hence the multifrequency spectra were obtained by dissolving the Cr(V/III)−citrate sample in DMSO saturated with picolinic acid. The X-band spectrum in DMSO (Figure 5b) is very similar to that obtained in water. The spectra in Figure 5 are plotted such that the gauss/mm is the same for spectra obtained at the three frequencies. Comparison of the spectra obtained at

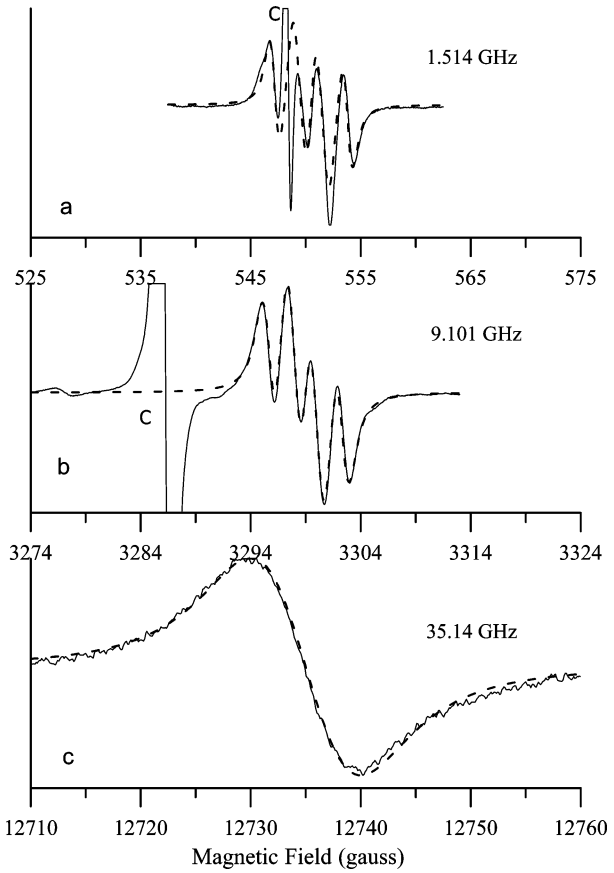

Figure 5. Room-temperature EPR spectra of $[CrO(caH_2)_2]^-$ plus excess picolinate in DMSO as a function of microwave frequency: (a) 1.514-GHz spectrum obtained with 0.34-mW microwave power and 0.10-G modulation amplitude; (b) 9.101-GHz spectrum obtained with 5-mW microwave power and 2.0-G modulation amplitude; (c) 35-GHz spectrum obtained with 3.7-mW microwave power and 1.0-G modulation amplitude. The simulated spectra (dashed lines) were obtained with $g_{iso} = 1.9715$, $A_N = 1.8 \times 10^{-4}$ cm^{-1}, and $A_H = 2.4 \times 10^{-4}$ cm^{-1}. The line widths were 1.514 GHz, 1.0 G; 9.101 GHz, 2.0 G; and 35.14 GHz, 8.0 G. The signal for $[CrO(caH_2)_2]^-$ is marked by "C" and was not included in the simulations.

1.514 and 9.101 GHz shows that the spacing, in gauss, between the lines of the four-line pattern is independent of frequency. If the four-line signal at X-band had been due to overlap of two three-line spectra with different g values, the separation between the two patterns would have decreased by a factor of 1.514/9.101 ∼ 0.17 when the microwave frequency was decreased, which is not consistent with the data. The frequency independence of the observed splitting shows that the additional splitting is due to coupling to a proton ($I = {}^1/_2$) and not to two species with different g values. The line widths of the signals are dominated by incomplete motional averaging of g and A anisotropy, and so the line widths increase with increasing microwave frequency. The line width at 35.14 GHz is so large that the nitrogen and proton hyperfine splitting is not resolved in the spectrum of $[CrO(caH)(pa)]^-$ (Figure 5c). The spectra at the three frequencies were simulated using the same g value and hyperfine splittings with adjustment of the line widths. The g value difference between the $[Cr^VO(caH_2)_2]^-$ starting material and $[CrO(caH)(pa)]^-$ causes a better separation of the EPR signals of the two species as the microwave frequency is increased, and at 35.14 GHz, the signal for

(69) Zhang, L.; Lay, P. A. *Inorg. Chem.* **1998**, *37*, 1729−1733.
(70) Carruthers, L. M.; Closken, C. L.; Link, K. L.; Mahapatro, S. N.; Bikram, M.; Du, J.-L.; Eaton, S. S.; Eaton, G. R. *Inorg. Chem.* **1999**, *38*, 3529−3534.

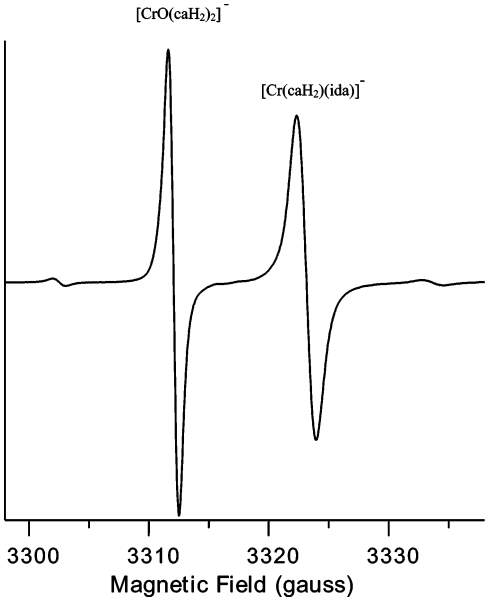

Figure 6. Room-temperature X-band (9.1712 GHz) EPR spectra of $[CrO(caH_2)_2]^-$ plus ida (100 mM, pH 4.2); the spectrum was obtained with 5-mW microwave power and 1.0-G modulation amplitude; mod. frequency, 100 kHz; gain, 0.1×10^4; scans, 3; sweep time, 30 s; time constant, 0.1280 s.

$[CrO(caH_2)_2]^-$ is sufficiently well separated from the signal for $[CrO(caH)(pa)]^-$ that it is not seen within the 50-G scan presented in Figure 5c. The spectrum of $[CrO(caH)(pa)]^-$ is the same in H_2O or D_2O solution, which shows that the unique proton coupling does not arise from a solvent-derived proton or an exchangeable O−H proton on the citrate ligand. The four-line EPR spectra in Figure 5 were essentially unchanged when the same experiments were performed in DMSO with the deuterated ligand (D_4C_5NCOOH); therefore, the unique proton must come from the citrate rather than from the picolinate.

At constant pH values and variable concentrations of paH (20−100 mM), the ratio of the Cr(V)−pa signal to the $[CrO(caH_2)_2]^-$ signal increased linearly with the [paH], which shows that the equilibrium involves 1 mol of picolinate per Cr(V), consistent with the observation of a coupling to a single nitrogen. In a mixture of $[CrO(caH_2)_2]^{2-}$ and picolinate, the loss of the EPR signals as a function of time for both $[CrO(caH_2)_2]^-$ and $[CrO(caH)(pa)]^-$ was monitored. They were best fitted to consecutive first-order processes, similar to those observed in the disproportionation of $[CrO(ehba)_2]^-$.[14] The first-order rate constants at 220.2 °C for the decay of $[CrO(caH_2)_2]^-$ are $(1.8 \pm 0.4) \times 10^{-2}$ and $(1.8 \pm 0.04) \times 10^{-3}$ s^{-1} and for $[CrO(caH)(pa)]^-$ are $(1.3 \pm 0.2) \times 10^{-2}$ and $(1.2 \pm 0.06) \times 10^{-3}$ s^{-1}. The data do not fit as well to first-order kinetics or to second-order kinetics. Typical plots are given in the SI (Figures S2 and S3).

The EPR spectra of Cr(V/III)−citrate in a solution of $idaH_2$ (ida = iminodiacetate) (100 mM, pH 4.0) showed a new signal at $g_{iso} = 1.971$, which is assigned to $[CrO(caH_2)(ida)]^-$ (eq 4) (Figure 6). Whether both the carboxylates of ida or only one of the carboxylates is ligated to the oxochromate-(V) center could not be discerned from the EPR results. If ida binds via only one carboxylate, the resulting mixed oxochromate complex would be neutral instead of the anionic complex that is shown in eq 4.

$$[CrO(caH_2)_2]^- + idaH \rightarrow [CrO(caH_2)(ida)]^- + caH_3 \quad (4)$$

The line width of the signal for the ida complex (1.8×10^{-4} cm^{-1}) indicates that if there is any ^{14}N-superhyperfine coupling, it must be less than $\sim 0.5 \times 10^{-4}$ cm^{-1}, which would be much smaller than the 1.8×10^{-4} cm^{-1} ^{14}N-superhyperfine splittings observed for the picolinate complex.

The equilibrium constants for ligand-exchange reactions with pa and ida (eqs 3 and 4) were calculated on the assumption that the concentration of ca released is equal to the equilibrium concentration of $[CrO(caH)(pa)]^-$ or $[CrO(caH_2)(ida)]^-$ that was determined from the normalized integral data for the mixed complex. At 22 °C, the values of K_{pa} lie in the range $(5.0 \pm 2.5) \times 10^{-3}$ while K_{ida} values are $(7.5 \pm 1.5) \times 10^{-4}$ (pH 4.0−4.5). The uncertainty in the estimated equilibrium constant values could be due to the following factors. First, quite unlike the ligand-exchange reaction of $[CrO(ehba)_2]^-$ with 1,2-ethanediol,[23] the decomposition of the mixed-ligand Cr(V) complexes occurred at significant rates. Second, the ligand-exchange equilibria may be influenced by ionic strength due to charge differences between the reactants and products. In ligand-exchange experiments involving picolinate, the ESMS of the product showed a dominant peak at $m/z = -363.2$, which is attributed to a mixed-ligand Cr(III) complex, **IV**, $[Cr(caH)(pa)]^-$, which is consistent with a mixed-ligand Cr(V) intermediate.

In reactions with either 2,2′-bipyridine or 1,10-phenanthroline (pH 4.1 ± 0.1), fast ligand-exchange and decomposition reactions of the resulting Cr(V) complexes containing one caH and one of the bidentate nitrogeneous bases were observed. The normalized integrals show that more than 80% of the initial Cr(V) decayed during the first 4 min after mixing. EPR spectra of the products (Figure 7) exhibited hyperfine splitting to two nitrogens plus an additional $I = {}^1/_2$ nucleus.

Discussion

The Structure of the Cr(V)−Citrate Complex. Taken together, the ESMS, UV−vis, XANES, and EPR (solid state and solution) results show that the solid designated as Cr(V/III)−citrate is a mixture of $[CrO(caH_2)_2]^-$ (**I**) and a

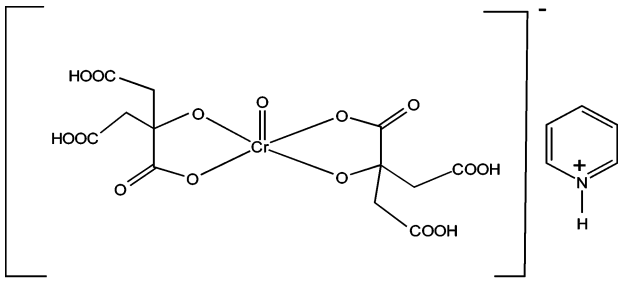

I

Cr(III) complex, which presumably is a bis(citrate) complex (**II**). The degree of protonation of the citrate in **II** is ambiguous. While the complex is designated as $[Cr(caH_2)(caH)]^{2-}$

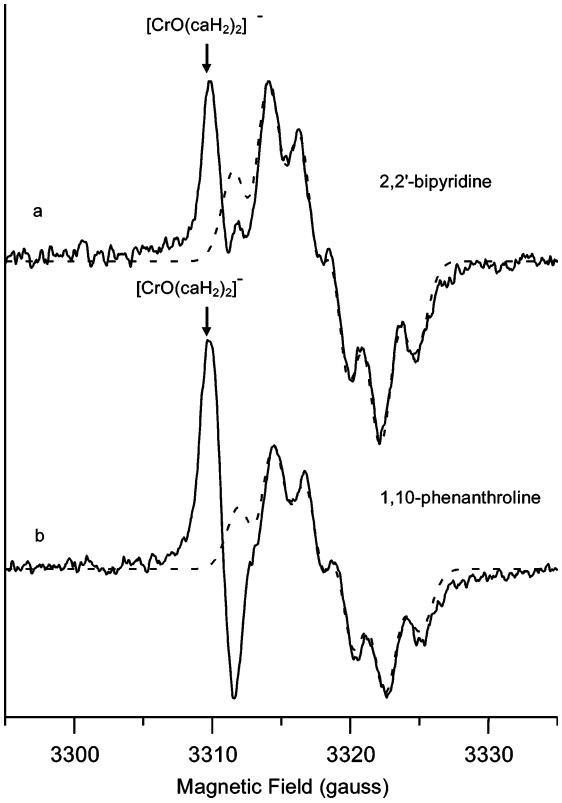

Figure 7. Room-temperature continuous-wave X-band (9.17 GHz) EPR spectra of aqueous solutions obtained with 5-mW microwave power and 2.0-G modulation amplitude. (a) The spectrum was recorded 2 min after 2,2′-bipyridine (100 mM) was added to a fresh sample of **I** (1 mg mL^{-1}) in water at pH 4.0. (b) The spectrum was recorded 2 min after 1,10-phenanthroline (100 mM) was added to a fresh sample of **I** (1 mg mL^{-1}) in water at pH 4.0. The simulated spectra (dashed lines) were obtained with $g_{iso} = 1.9729$ (a) or $g_{iso} = 1.9744$ (b), and nitrogen hyperfine coupling to two inequivalent nitrogens with $A_N = 1.8 \times 10^{-4}$ cm^{-1} and 2.6×10^{-4} cm^{-1}, and coupling to a unique proton with $A_H = 2.2 \times 10^{-4}$ cm^{-1}. The ^{53}Cr satellite lines and the signal for $[CrO(caH_2)_2]^-$ were not included in the simulations.

based on the ESMS data, the level of protonation is difficult to determine from ESMS, and the XAFS structure is more consistent with $[Cr(caH_2)_2]^-$. In the EPR spectrum, the zero-field splitting for $(pyH)_2[Cr(caH_2)(caH)]\cdot 4H_2O$ is about 1 cm^{-1} with rhombicity (E/D) = 0.29;[49] such a large zero-field splitting means that the positions of the lines are strongly dependent upon small changes in geometry at the metal center. The broader lines for the Cr(III)−citrate complex in the Cr(V/III)−citrate solid than in pure $(pyH)_2[Cr(caH_2)(caH)]\cdot 4H_2O$ (Figure 4) may reflect wider distributions in zero-field splittings in the mixture than in the pure solid or may be due to the presence of $[Cr(caH_2)_2]^-$ (see XAFS results). Irrespective of the degree of protonation, the results are consistent with this Cr(III) species being in the solid sample. Apparently, the mixed salt containing the Cr(V) and Cr(III) complexes is much less soluble in acetone than the individual components. The instability of the Cr(V) complex in solution has prevented the separation of the Cr(V) species from the Cr(III) species using chromatography, to date, but the Cr(V/III) citrate is stable for months in the solid state in which Cr(V)−citrate constitutes 25−35% of Cr content.

Ligand-Exchange Chemistry of $[CrO(caH_2)_2]^-$. While the $[CrO(caH_2)_2]^-$ complex is short-lived in aqueous solution, it is a convenient starting material for ligand-exchange reactions. In view of the demonstrated reluctance on the part of $[CrO(ehba)_2]^-$ to undergo ligand-exchange reactions with nitrogen donor ligands,[3] the ligand-exchange studies with $[CrO(caH_2)_2]^-$ are important because this starting material permits formation of complexes with nitrogen donors including picolinate, 2,2′-bipyridine, and 1,10-phenanthroline. The monopicolinate stoichiometry was confirmed by EPR spectroscopy and by examination of the composition of the Cr(III) end product by electrospray mass spectrometry. The ^{14}N hyperfine splitting ($A_{iso}(N) = 1.8 \times 10^{-4}$ cm^{-1}) for the Cr(V) picolinate complex is similar to that observed for nitrogens bound equatorially to d^1 vanadyl,[72] which like Cr(V) has a single unpaired electron in the d_{xy} orbital. Electron spin−echo envelope modulation studies of vanadyl complexes have shown that axially bound nitrogen has a coupling constant of about 0.5×10^{-4} cm^{-1},[72] which suggests that a similar magnitude of hyperfine interaction might be found for nitrogen bound axially to Cr(V). Thus the absence of resolved nitrogen hyperfine in the spectrum of $[CrO(caH_2)(ida)]^-$ indicates that there is not an equatorially coordinated nitrogen, but the possibility of axially coordinated nitrogen cannot be ruled out.

The $[CrO(caH)(pa)]^-$ complex was characterized as a six-coordinate complex, **III**, on the basis of g_{iso} value (the calculated value for this structure is 1.9701),[71] the ^{53}Cr hyperfine coupling (18.4×10^{-4} cm^{-1}), and the observation of strong superhyperfine coupling to a unique C−H proton on the citrate. The latter, in particular, shows that part of the aliphatic backbone of the citrate must be in close proximity to the Cr center, consistent with a six-coordinate structure. It is apparent that replacing a 2-hydroxy acid donor with a weaker donor, such as pa, results in the formation of a six-coordinate complex in which the remaining citrate

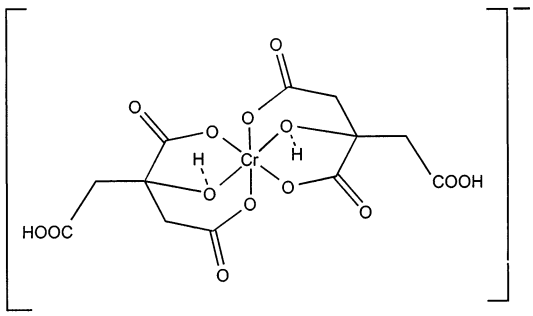

II

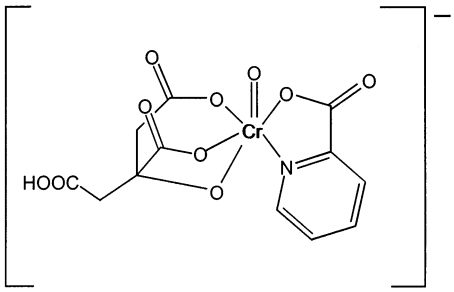

III

Scheme 1

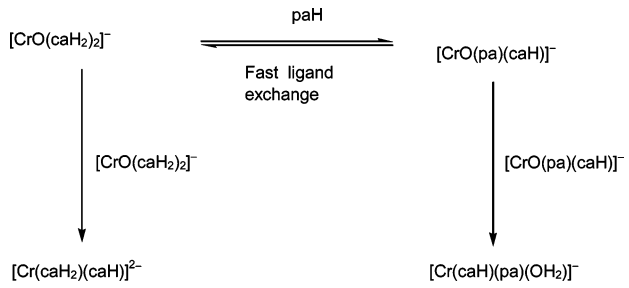

becomes tridentate to compensate for the weaker N donor compared to the deprotonated alcohol donor in the ehba complex.

The ESMS evidence for the presence of the mixed-ligand Cr(III) product, **IV** ($[Cr^{III}(caH)(pa)]^-$, or a similar structure with the alcoholato donor replacing a carboxylato donor), in the ligand-exchange experiments involving picolinate is consistent with the proposed equilibrium in the Cr(V) oxidation state. Both the observed EPR spectra and bimolecular kinetics predict the structure of the final reduction product to be a mixed-ligand complex. If the reaction were to involve unimolecular decomposition of **III**, the reduction to Cr(III) would involve the oxidation of the bound citric acid rather than picolinic acid due to the well-known inertness of pa toward oxidation. To the best of our knowledge, this is the first report of a mixed-ligand Cr(III) complex containing citrate and picolinate. This is significant given the current flurry of activity involving Cr(III) picolinate as a dietary supplement[73] and the controversial role of Cr-(III) in glucose and fat metabolism.[71,74]

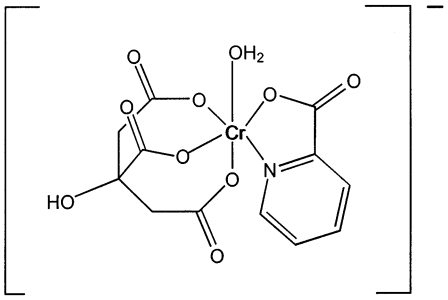

IV

The decomposition of both $[CrO(caH_2)_2]^-$ and $[CrO(caH)(pa)]^-$ follows consecutive first-order kinetics with respect to [Cr(V)], which is similar to the behavior observed for $[CrO(ehba)_2]^-$.[14] Scheme 1 shows that the ligand-exchange reaction is fast relative to the subsequent decay of the Cr(V)−citrate or the Cr(V)−picolinate complex. While detailed mechanistic studies have not been performed, the similarity in the kinetics with those observed for $[CrO(ehba)_2]^-$ [14] suggests similar mechanisms.

The structures of the mixed-ligand phen and bpy complexes are clearly different from one another as evidenced by the different g_{iso} values. The g_{iso} value of the bpy complex is consistent with a six-coordinate bis(oxo) bipy complex, $[Cr(O)_2(caH_2)(bipy)]^-$, **V** (calcd $g_{iso} = 1.9725$, obsd 1.9729),[71]

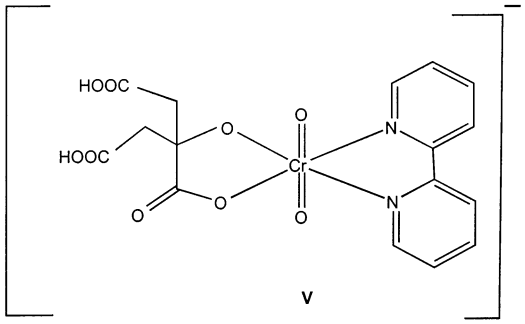

and a five-coordinate phen complex, $[CrO(caH_2)(phen)]^+$, **VI** (calcd $g_{iso} = 1.9746$, obsd 1.9744).[71] These differences

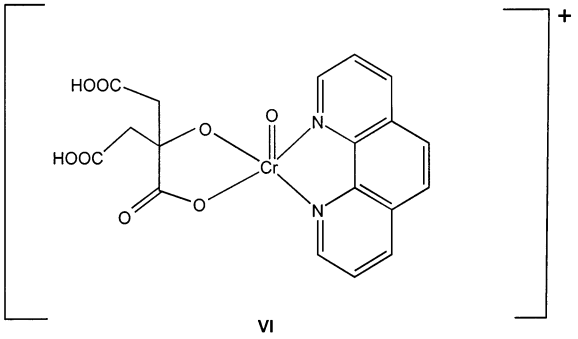

in g_{iso} values are similar to differences between five- and six-coordinate oxochromate(V) complexes that are in slow equilibrium on the EPR time scale.[25,71] Like the pa complex, the bipy complex prefers to coordinate a sixth strong ligand donor to compensate for the weak donor properties of the aromatic imine. Apparently, the more sterically demanding phen ligand prevents the formation of an analogous six-coordinate phen species as was observed for the bipy complex, although these species need to be characterized further before definitive structures can be assigned.

The g_{iso} value of 1.971 for the ida complex provides strong evidence that the ida complex has a similar structure as the pa complex, g_{iso}(calcd) = 1.9707, because amine and imine donors result in similar g_{iso} values.[71] Although it is not clear whether the sixth caboxylate ligand comes from the ida or ca ligand, it is more likely to come from the former, since no caH-derived ^{1}H superhyperfine coupling, like that observed in the pa complex, is observed in the ida complex.

Implications for Chromium Genotoxicity. The current results show that Cr(V) can be stabilized by the biologically relevant 2-hydroxy acid ligand, citric acid, in a similar manner as the much-studied ehba and hmba complexes. The fact that such a ligand can stabilize Cr(V) en route to

(71) Levina, A.; Codd, R.; Dillon, C. T.; Lay, P. A. *Prog. Inorg. Chem.* **2003**, *51*, 145−250. Calculations were performed using the following empirical parameters for Δg_{iso}: $O^{2-} = -0.00210$; $RO^- = -0.00505$; $RCO_2^- = -0.00593$; $R_3N = -0.00667$; $R_2C{=}NR = -0.0073$; and $g_{iso}(calcd) = 2.0023 + \Sigma\Delta g_{iso}$. This equation has recently been shown to predict the g_{iso} values of a range of well-characterized Cr(V) complexes.

(72) Lobrutto, R.; Hamstra, B. J.; Colpas, G. J.; Pecoraro, V. L.; Frasch, W. D. *J. Am. Chem. Soc.* **1998**, *120*, 4410−4416.

(73) Evans, G. W.; Pouchnik, D. J. *J. Inorg. Biochem.* **1993**, *49*, 177−187.

(74) (a) Vincent, J. B. *Polyhedron* **2001**, *20*, 1−26. (b) Stearns, D. M. *BioFactors* **2000**, *11*, 149−162.

reduction of carcinogenic Cr(VI) to Cr(III), shows that such species may be generated in vivo. The similarity in the ligand-exchange chemistry also shows that this complex has the potential to damage DNA in the same manner as that reported by the hmba and ehba analogues at the two pH values of relevance to Cr(VI)−induced cancers (i.e., 7.4 and 3−5).[5−7,14,15]

Acknowledgment. The support of this work by Research Corporation (S.N.M.; Cottrell College Science Award C-2816) is gratefully acknowledged. We are grateful to Professor Jan Roček, retired Vice Chancellor for Research, University of Illinois, Chicago, for his initial inspiration for this work. We thank Dr. Robert Barkley, Jr., and Ms. Olga Averin of the Central Analytical Laboratory at the University of Colorado, Boulder, for the electrospray mass spectra and Dr. Mark Panda, Department of Biochemistry, University of Texas Health Sciences Center at San Antonio, Texas, for kinetic analyses. The XAS work was performed at the Australian National Beamline Facility (ANBF) with support from the Australian Synchrotron Research Program, which is funded by the Commonwealth of Australia under the Major National Research Facilities program. The authors thank Drs. James Hester (ANBF) and Colin Weeks (University of Sydney) for assistance with the XAS experiments. We are also grateful for support from an Australian Research Council Large Grant (P.A.L.) and ARC RIEFP grants for the 10-element Ge detector at ANBF and for the EPR spectrometers at the University of Sydney.

Supporting Information Available: Conditions applied to the MS XAFS fittings for the Cr(V)−Cr(III)−citrate mixture; initial, restrained, and optimized parameters of MS XAFS fitting for the Cr(V)−Cr(III)−citrate mixture; major pathways in the MS analysis; model used for MS XAFS calculations for the Cr(V)−Cr(III)−citrate mixture; application of window functions to MS XAFS calculations for the Cr(V)−Cr(III)−citrate mixture; and consecutive first-order reaction fits to the kinetic data for ligand-exchange reactions. This material is available free of charge via the Internet at http://pubs.acs.org.

IC034146L